Multi-variable optimization
of an ytterbium-doped fiber laser
using genetic algorithm

Somaye Sadat HASHEMI, Saeed GHAVAMI SABOURI[*], Alireza KHORSANDI

Department of Physics, University of Isfahan,
Hezar Jarib Street, Isfahan 81746-73441, Iran

[*]Corresponding author: ghavami@sci.ui.ac.ir

We introduce the genetic algorithm for the optimization of an Yb^{3+}-doped double-clad fiber laser based on a multi-variable scheme. The output characteristic of the laser is numerically simulated using real practical values. This is performed through solving the associated steady-state rate equation and investigating the effects of input variables such as pump and signal wavelengths and length of the fiber on the laser output. It is found that pumping of the medium around 975 nm is conducted to attain the maximum output power of ~34.8 W, while the stability of the outcoupled power is significantly improved when pumping at 920 nm, confirming good agreement with the reported experimental results. We have also found that by using genetic algorithm base multi-variable optimization, the output power can be significantly increased by about three orders of magnitude and reaches to ~28.5 W with optimum and shorter fiber length of ~57.5 m. Obtained results show that based on the genetic algorithm multi-variable discipline, fiber characteristics can be optimized according to the gaining of maximum output power.

Keywords: fiber laser, optimization, genetic algorithm.

1. Introduction

Owing to the unique properties of high-power fiber lasers, including high conversion efficiency, excellent beam quality, low thermal effects as well as small physical size and weight, they replace other conventional laser sources for numerous applications in medicine [1] defence [2], industrial processing [3] and modern telecommunication [4]. Recently, ytterbium-doped double-clad fiber lasers have attracted considerable attention because they benefit from a relatively broad fluorescence bandwidth (>150 nm), which is quite appreciable for the applications which require tunable laser sources [5, 6]. The energy system of the Yb^{3+} ion is quasi-three-level which makes the excited-state absorption of pump and signal beams quite negligible provided that the laser efficiency is significantly high [7]. Moreover it has a large absorption cross-section around 980 nm band where low-cost and high power diode lasers are commercially available

for employing them as a favorable pump source in the entire absorption band of an Yb^{3+}-doped fiber [8]. However, it is found that the laser performances such as output power stability and optical efficiency are strongly dependent on the operating wavelength of the utilized pump source [9]. On the other hand, by precisely stabilizing and adjusting the pumping wavelength, Yb^{3+}-doped fiber laser is capable of lasing at different wavelengths. In this regard, several schemes have been demonstrated for multi-wavelength operation, for example, by using two Sagnac loop mirrors inside the cavity [10]. This guarantees that pumping and lasing wavelengths lie in quite different spectral regions even with low absorption and emission cross-section of Yb^{3+} ion. The feasibility of using Yb^{3+} fibers with a double-clad scheme is recently investigated as the promise choice for high power laser sources in different applications which may require a compact and robust fiber format. The performance of a double-clad fiber laser is associated with many dependent variables that can be simultaneously optimized through using the steady-state rate equations with particular attention to the fiber length and operating pump and signal wavelengths which are prior to any experimental setups. Much of the research efforts have been established on a common assumption in which the absorption and emission cross-sections are wavelength-independent parameters [11–13]. However in practice those have been introduced as sensitive variables to the operating wavelengths and surrounding environment as well. Therefore, the optimum performance of a typical double-clad fiber laser needs a multi-variable optimization algorithm. The genetic algorithm (GA) is known as search heuristic that simulates the process of natural selection to generate useful solutions to optimization of multi-variable problems [14]. It has widely found application in different areas of optics and lasers [15–17] where by routine methods simultaneous solving of multi-variable equations is impossible. The GA is based on the generation of a large population which can be mutated and altered toward better solution. The generated population contains a certain number of "individuals", each has a set of properties which are described by a coded datum called "chromosome". Once the initial population is generated, the evolution continues with an iterative process including selection, crossover and mutation to produce a new generation. The best individuals are then randomly selected from the current population to produce another generation and next iteration of the algorithm is started again. After many consecutive generations, the iteration terminates when a satisfactory performance has been reached for the population [18]. In the case of fiber optimization, chromosomes are fiber length and operating pump and signal wavelengths. Despite impressive achievements reported in literature, optimization of a fiber laser with pump and signal wavelengths and fiber length as variables has not been performed yet [12, 19].

In this work, for the first time to our knowledge, based on the multi-variable GA discipline, the performances of a typical Yb^{3+}-doped fiber laser are characterized and optimized by setting the pump and signal wavelengths and fiber length as optimization variables. This is performed through numerical solving of the associated stand-

ard steady-state rate equations using real practical values. The motivation of using the GA is the maximizing of the output power while keeping the fiber length and operating wavelengths as dependent variables. The dependence of the optimum pump and signal wavelengths and fiber length as well as the doping concentration of the Yb^{3+} and scattering loss on the laser output power have been accordingly discussed and analyzed. Our results on optimizing the fiber length and operating wavelengths with GA provide very useful guidelines prior to the experiment with the attainment of highest output power. The process is repeated for different levels of Yb^{3+} concentrations and scattering losses and associated results are extracted from the presented plots.

2. Theoretical model

We start by the fact that when the pumping level is strong enough, the effect of amplified spontaneous emission (ASE) is quite negligible [12] and therefore can be ignored. Here, a numerical method is used to solve the rate equations of a laser in a steady-state regime. Eventually, the rate equations of a typical rare-earth-doped double-clad fiber laser can be described as [20]

$$\frac{N_2(z)}{N_0} = \frac{\dfrac{[P_p^+(z) + P_p^-(z)]\sigma_{ap}\Gamma_p}{h\upsilon_p A} + \dfrac{[P_s^+(z) + P_s^-(z)]\sigma_{as}\Gamma_s}{h\upsilon_s A}}{\dfrac{[P_p^+(z) + P_p^-(z)](\sigma_{ap} + \sigma_{ep})\Gamma_p}{h\upsilon_p A} + \dfrac{1}{\tau} + \dfrac{[P_s^+(z) + P_s^-(z)](\sigma_{as} + \sigma_{es})\Gamma_s}{h\upsilon_s A}}$$

(1)

$$\pm\frac{\mathrm{d}P_p^\pm(z)}{\mathrm{d}z} = -\Gamma_p[\sigma_{ap}N_0 - (\sigma_{ap} + \sigma_{ep})N_2(z)]P_p^\pm(z) - \alpha_p P_p^\pm(z)$$

(2)

$$\pm\frac{\mathrm{d}P_s^\pm(z)}{\mathrm{d}z} = -\Gamma_s[\sigma_{as}N_0 - (\sigma_{as} + \sigma_{es})N_2(z)]P_s^\pm(z) - \alpha_s P_s^\pm(z) +$$

$$+\Gamma_s\sigma_{es}N_2(z)2hc^2\frac{\Delta\lambda_s}{\lambda_s^3}$$

(3)

where $P_p(z)$ and $P_s(z)$ are the pump and signal powers, respectively, with the associated forward $P^+(z)$ and backward $P^-(z)$ powers; $\sigma_{ap/ep}(\lambda_p)$ and $\sigma_{as/es}(\lambda_s)$ are the wavelength-dependent absorption and emission cross-section of pump and signal beams, respectively; τ is the lifetime of spontaneous photons; $N_2(z)$ is the population density of the upper laser level; N_0 is the density of Yb^{3+} dopant; $\Delta\lambda_s$ is the signal bandwidth which is assumed ~9 nm throughout the simulation; A is the effective area of the fiber
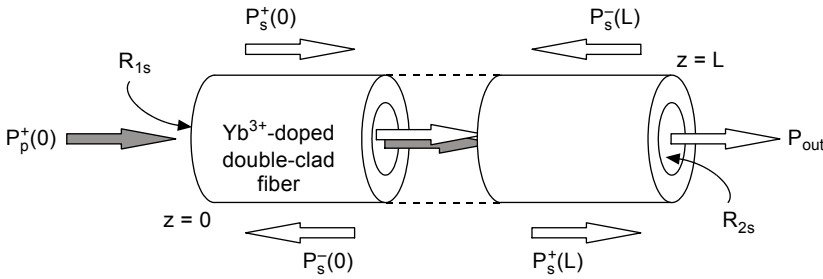
Fig. 1. Pumping scheme of a lengthy Yb^{3+}-doped double-clad fiber laser. By assuming $P_p^-(L) = 0$ the backward pumping is ignored.

core and $\Gamma_{p/s}$ and $\alpha_{p/s}$ are the filling factor and scattering loss of the pump and signal waves, respectively. The physical situation is schematically shown in Fig. 1. The required boundary conditions for the laser power are determined by the following expressions:

$$P_s^+(0) = R_{1s} P_s^-(0) \tag{4a}$$

$$P_s^-(L) = R_{2s} P_s^+(L) \tag{4b}$$

where R_{1s} and R_{2s} are forward and backward reflectivities at the laser wavelength which in our investigation are assumed 4% and 98%, respectively.

It is further assumed that the fiber ends are completely transparent for the pumping wavelength and hence $P_p^-(L) = 0$. As long as the input variables such as pumping and signal wavelengths as well as fiber length are optimally determined, the contribution of $P_s^+(z)$ and $P_s^-(z)$ to the generated power along the z-axis can be evaluated and numerically simulated for real experimental data. The optimum pumping region de-
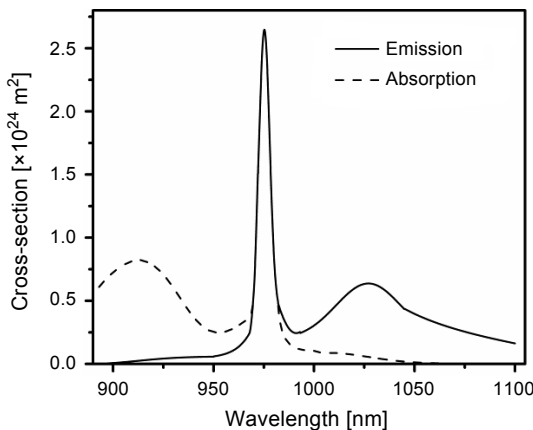

Fig. 2. Digitized absorption and emission cross-sections, σ_a and σ_e, of the Yb^{3+} which is obtained through fitting mathematical functions into the experimental curves reported in [12]. The regenerated plot gives the data with an accuracy of better than 0.1% when compared with the real values.

pends on the spectral feature of absorption and emission cross-sections, σ_a and σ_e, of the Yb^{3+} ion. In Figure 2 the required pieces of information are extracted through digitizing the measured data reported in [12]. This is performed by fitting the appropriate functions into the experimental curves.

As can be seen from the plot, σ_a shows two maximums about 920 and 975 nm. The same trend can be observed for σ_e at 975 nm with a very sharp peak, while around 1027 nm it benefits from a relatively smooth curvature, making it very advantageous for the generation of laser radiation in a relatively wide range of possible wavelengths far away from the pumping region.

3. Optimization of fiber laser performance: results and discussion

We follow the procedure through maximizing the laser efficiency with respect to the input parameters. It is performed by taking pumping and laser wavelengths and fiber length as initial variables while Yb^{3+} concentration and pump power were set at desirable values. Therefore, the optimum performances like pumping and laser wavelengths can be attained through numerical solving of Eqs. (1) to (3) while we assumed the absorption and emission cross-sections are variables. Such a multi-variable problem which to the best of our knowledge is performed for the first time is the subject of GA technique that is executed in MATLAB GA toolbox. For making the consistency with the experimental data, we have assumed that $\Gamma_p = 0.0012$, $\Gamma_s = 0.82$ and $A = 5 \times 10^{-7}$ cm^2 throughout this work [12]. Figure 3 illustrates the results of simulation for the laser output power *versus* fiber length. The GA solution is also given to indicate how the optimum length can be obtained for different scattering losses. The plot confirms that for greater scattering losses the optimum fiber length is decreased and
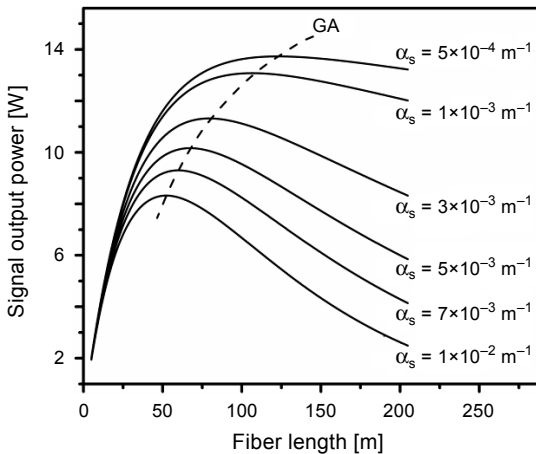

Fig. 3. Variation of the signal output power with fiber length for different scattering losses (solid lines). The optimized fiber length obtained by GA solution is specified by the dashed line. Pump power and Yb^{3+} concentration are assumed 20 W and 4×10^{25} m^{-3}, respectively.

the output power seems more sensitive to the fiber length. This can be explained by the fact that stimulated photons and scattering loss are in competition with each other where due to the scattering for longer fibers, larger number of induced photons will be lost. Therefore, to decrease the power dissipation, shorter fiber length is preferred. In contrast, approaching higher signal power is necessarily achieved through using longer length and thus GA solution shows that for gaining optimum performance those two effects must be properly balanced. However, obtained results shown in Fig. 3 confirm that the GA is capable enough to find an optimum fiber length while the maximum output power is preserved for each level of scattering loss. As long as the optimum fiber length is determined, the second variable can be arrived into the optimization loop for the same amount of scattering losses. Next we consider the effect of signal wavelength on the output power within 980 to 1100 nm range. Using the simulation results deduced in Fig. 3, the optimum signal wavelength can be evaluated by running the GA technique. Obtained results are shown in Fig. 4. As can be seen, while the scattering loss is decreased, the maximum of the output power is increased. Indeed, for low loss and longer fibers the optimum signal wavelength is sustained by a red shift of about 6.5 nm where for the scattering losses varying from 1×10^{-2} to 5×10^{-4} m^{-1} the optimum signal wavelength is changed from 1066.5 to 1073 nm, respectively.
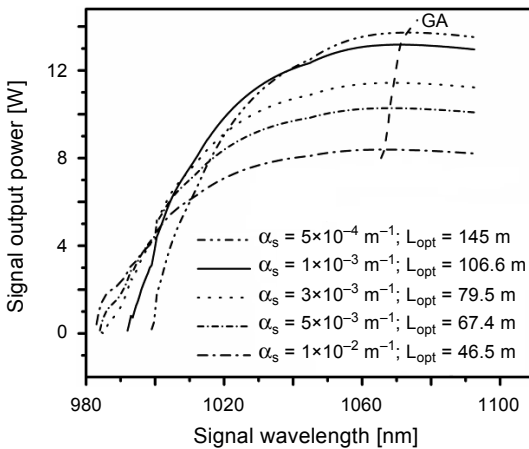

Fig. 4. Output power variation with a relatively wide range of signal wavelength while the optimum length of fiber and corresponding scattering loss are acquired from Fig. 3 with similar pump power and Yb^{3+} concentration.

This relatively large shift indicates that the fiber performance is very susceptible to the optimum operating signal wavelength, confirming the significance of our presented GA-based multi-variable optimization process.

So far two variables have been investigated and to account for the next one, we introduce the pumping wavelength. Regarding the obtained results shown in Figs. 3 and 4, the influence of pump wavelength on the output power is evaluated and numerically simulated in Fig. 5.
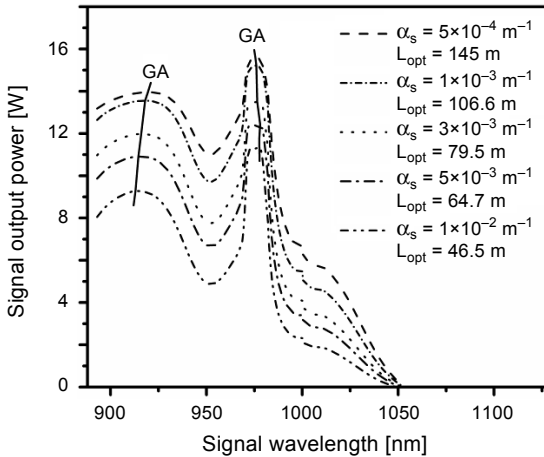
Fig. 5. Variation of signal output power in a relatively wide range of pump wavelengths for the same parameters as used in plotting Fig. 3. Solid line shows the optimal values obtained from GA solution. The optimum lengths at corresponding scattering losses are extracted from the results shown in Fig. 3. Signal wavelength is assumed 1090 nm.

As clarified in the plot, the optimum pump wavelength is located between 977.6 and 975 nm range when the scattering loss in accordingly changed from 1×10^{-2} to 5×10^{-4} m^{-1}, respectively. Referred to Fig. 2, since the maximum of absorption cross-section σ_a occurs at 975 nm it is quite reasonable to conclude that the active medium is potentially capable of absorbing most of the pump energy at the same wavelength. On the contrary, displayed results illustrated in Fig. 5 indicate that the optimum wavelength is strongly dependent on the scattering loss inside the medium where for higher losses optimal point is displaced toward longer pump wavelengths. However, despite the severe dependence of the output power on pumping wavelength, the optimum circumstances can be lost by the variation of the energy loss within the fiber. This again underlines the significance of the presented optimization method in designing an efficient fiber laser. Based on the GA solution, we develop the procedure through calculating the optimum pump wavelength within two maximum bandwidths of the absorption cross-section characterized in Fig. 2. In the first one, the pump wavelength is changed from 912 to 919.5 nm while in the second, the maximum band pump wavelength varies from 970 to 980 nm. In both bands the scattering losses are assumed to change systemically from 1×10^{-2} to 5×10^{-4} m^{-1}. Although for the first band the calculated output power is about 12% less than that of the second pumping region, the laser output is more stable even though the input pump fluctuation is dominant.

Experimental results show similar achievements where as reported close to the first pumping maximums the output power stability is raised [9]. Therefore it is quite adequate to define a criterion for output power instability as the displacement of the power from its maximum point with taking into account the obtained optimum parameters. Figure 6 shows the ordinary numerical solution for the above instability for two maximums of pumping wavelength.
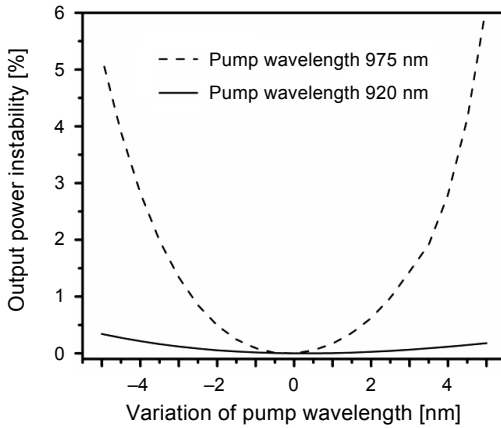
Fig. 6. Simulated output power instability while the pump wavelengths are displaced from their maximums. Calculation is performed for 920 and 975 nm. The scattering loss and optimum fiber lengths are assumed 5×10^{-4} m^{-1} and 145 m, respectively.

As evident in the figure, by a displacement of about ±5 nm from those maximum peaks, the instability is almost increased. The plot confirms that for 975 nm of pumping wavelength, the output power instability reaches to ~5%, and for shorter wavelength it rapidly declines and tends to a negligible value of ~0.04%. This is quite in agreement with the experimental results reported in [9].

The aim of using GA method in the present work is the optimization of signal wavelength and fiber length around the maximum output power while other parameters of the fiber like Yb^{3+} doping level and dissipative losses remain unchanged. In solving such a multi-variable problem the former are assumed as input variables while the pumping wavelength is scanned over a certain range from 900 to 980 nm. Figure 7 shows the results in which the maximum output power is accordingly determined. Referred to Fig. 5, the calculated output power included two band maximums. The first one was between 900 and 930 nm of pumping wavelength with about 27.5 W while the next occurred nearly at 975 nm with 34.8 W of output power. Although a similar trend can be observed in both Figs. 5 and 7, however, several remarkable points are:

– Figure 5 is based on one-variable optimization while multi-variable discipline is used in plotting Fig. 7.

– In the first maximum zone in Fig. 5 the output power is peaked at ~10.9 W for the optimum length of 64.7 m but in Fig. 7 it reaches ~28.5 W for the optimum length of ~57.5 m.

– In Fig. 5 the maximum output power at 975 nm of pumping wavelength and optimum fiber length of 64.7 m is ~12.4 W whereas in Fig. 7 we found 38.4 W for a much shorter length of ~26 m.

The above comparison shows that with multi-variable optimization it is quite possible to attain maximum output power at a proper length of Yb^{3+}-doped fiber which shows GA optimization method to be a promising candidate in terms of efficiency and
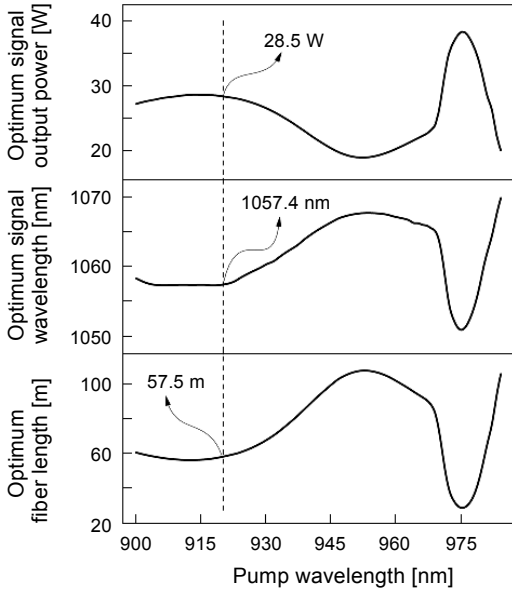
Fig. 7. Maximized output power at each corresponding pump wavelength while crossing the optimum curves of signal wavelength and fiber length. Dashed line is shown as an example to indicate how the obtained results can be used in optimizing the utilized Yb^{3+}-doped fiber laser around the maximum output power. The pump power, scattering loss and Yb^{3+} concentration are assumed 50 W, 5×10^{-3} m^{-1} and 4×10^{25} m^{-3}, respectively.
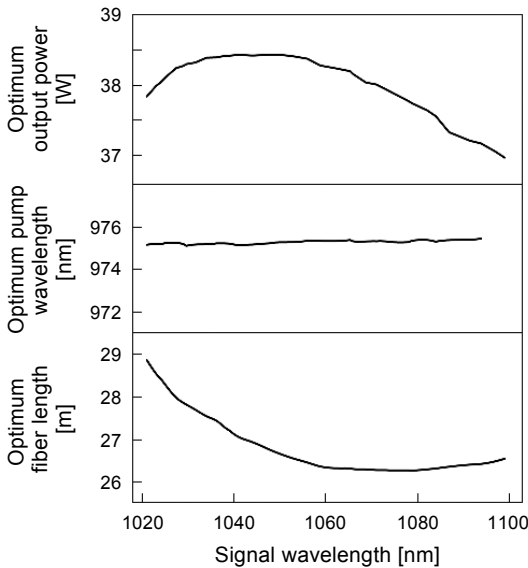

Fig. 8. Variation of the Yb^{3+}-doped output power with operating signal wavelength while both fiber length and pump wavelength are assumed as initial variables for GA environment. The pump power, scattering loss and Yb^{3+} concentration are assumed 50 W, 5×10^{-3} m^{-1} and 4×10^{25} m^{-3}, respectively.

very cost-effective technique. This again confirms that the use of GA method is re-
sponsible for obtaining a desirable output in a multi-variable scheme. The next impor-
tant feature of the calculation shown in Fig. 7 is that the efficiency of the generated
ytterbium laser is strongly dependent on the pumping wavelength where in the range
of 935 to 970 nm it is decreased even though the fiber length is designated relatively
long. As illustrated in Fig. 8, the above problem can be followed in a different manner
where pump wavelength and fiber length are assumed as input variables while the sig-
nal wavelength is scanned over a certain range to obtain the maximum output power.
As evident in the figure, the maximum output power can reach ~38.4 W within a signal
wavelength range of 1030 to 1055 nm at mostly constant pump wavelength close
to 975 nm. To further indicate the capability of GA technique, as a final step, preceding
constant parameters like Yb^{3+} concentration and scattering loss can be systematically
added to the simulation as initial variables to attain maximum output power. Figures 9
and 10 show the results of fiber optimization provided by GA solution in which the
new added variables have been scanned over a particular range.

   As can be seen from the plot, beyond 3×10^{25} m^{-3} of Yb^{3+} concentration, the output
power is not significantly increased and tends to almost constant value of ~16.8 W.
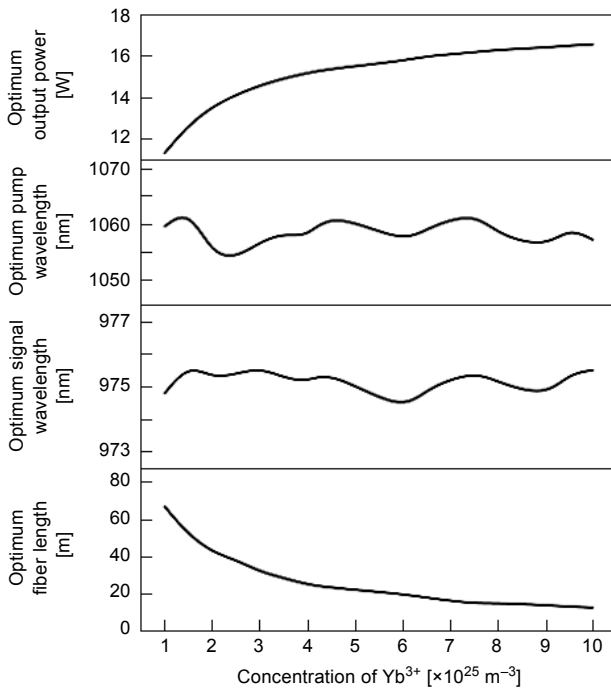As it is clear, the optimum pump wavelength is located around 975 nm, the second peak

Fig. 9. Optimum characteristics of the Yb^{3+}-doped fiber laser. It is performed by the variation of Yb^{3+}
concentration within a proper range and taking other parameters like fiber length, pumping and signal
wavelengths as input variables in GA. The pump power and scattering loss are 50 W and 5×10^{-3} m^{-1},
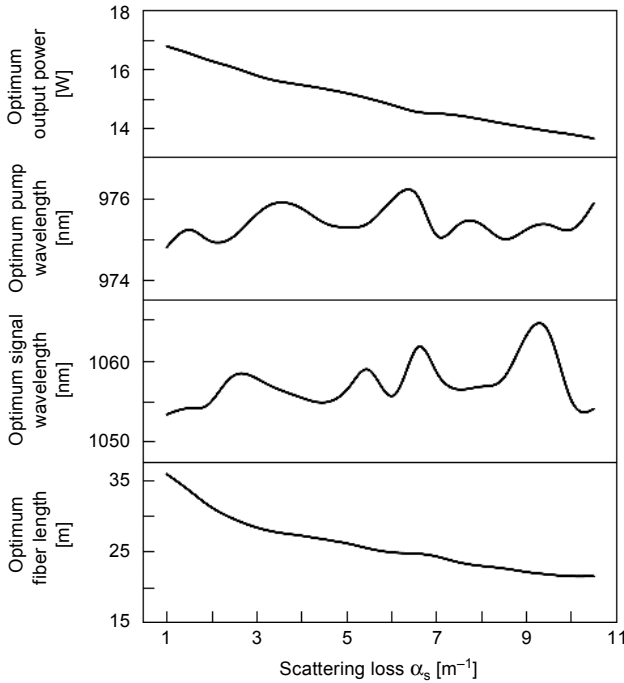respectively.

Fig. 10. Optimum characteristics of the Yb^{3+}-doped fiber laser. It is performed by the variation of scattering loss within a proper range and taking other parameters like fiber length, pumping and signal wavelengths as input variables in GA. The pump power and Yb^{3+} concentration are 50 W and 4×10^{25} m^{-3}, respectively.

of absorption cross-section is specified in Fig. 2, again confirming the consistency between the results. Moreover, the optimum signal wavelength is in 1054 and 1062 nm range away the maximum peak of emission cross-section indicated in Fig. 2. The main reason is that close to the peak wavelength of emission cross-section generated photons will be significantly absorbed. Finally, as shown in Fig. 10, the Yb^{3+} concentration is replaced by the scattering loss while the same procedure is performed for the fiber optimization. As evident in the figure, the optimum output power is a decreasing function of scattering loss. Similar to Fig. 9 we found that the optimum pump wavelength is around 975 nm while the optimum signal wavelength is varying from 1053 to 1065 nm.

4. Conclusion

In this paper, we have investigated the effect of pump and signal wavelength as well as fiber length, Yb^{3+} concentration and scattering loss on the output power based multi-variable solution using GA technique. This is performed by the optimization of fiber laser performance and earning the optimum parameters regarding the maximum attainable output power. To the best of our knowledge, for the first time GA discipline is used for multi-variable optimization of a typical Yb^{3+}-doped double-clad fiber laser.

Obtained results show that the optimum fiber laser parameters are strongly dependent on pump and signal wavelengths. It is found that for 920 and 975 nm of pumping wavelengths the output power reaches to its maximum values as 28.5 and 34.8 W, respectively. Moreover, despite a higher output efficiency at 975 nm, the fiber output stability at 920 nm is significantly increased which is in good agreement with the reported experimental results. It is further shown that the multi-variable solution based on the GA method enables to improve the optimization of fiber laser performances more efficient than the single-variable scheme. For example, in a single-variable solution when the pump wavelength is taken as an initial variable, the maximum of the output power reaches its peak at ~10.9 W for the optimum length of ~64.7 m while in the GA-based multi-variable optimization it reaches to ~28.5 W for the optimum length of ~57.5 m. It is further indicated that further increasing of Yb^{3+} concentration beyond 3×10^{25} m^{-3} does not increase the output power more than 16.8 W. In contrast, the output power shows to be quite susceptible to the inherent scattering losses. In summary, based on the GA multi-variable scheme gaining the optimum characteristics such as pump and signal wavelengths as well as fiber length is simultaneously possible.

References

[1] Sumiyoshi T., Sekita H., Arai T., Sato S., Ishihara M., Kikuchi M., *High-power continuous-wave 3- and 2-μm cascade Ho^{3+}:ZBLAN fiber laser and its medical applications*, IEEE Journal of Selected Topics in Quantum Electronics **5**(4), 1999, pp. 936–943.

[2] Hecht J., *Solid-state high-energy laser weapons*, Optics and Photonics News **14**(1), 2003, pp. 42–47.

[3] Kawahito Y., Terajima T., Kimura H., Kuroda T., Nakata K., Katayama S., Inoue A., *High-power fiber laser welding and its application to metallic glass $Zr_{55}Al_{10}Ni_5Cu_{30}$*, Materials Science and Engineering: B **148**(1–3), 2008, pp. 105–109.

[4] Mizrahi V., DiGiovanni D.J., Atkins R.M., Grubb S.G., Yong-Kwan Park, Delavaux J.M.P., *Stable single-mode erbium fiber-grating laser for digital communication*, Journal of Lightwave Technology **11**(12), 1993, pp. 2021–2025.

[5] Pask H.M., Carman R.J., Hanna D.C., Tropper A.C., Mackechnie C.J., Barber P.R., Dawes J.M., *Ytterbium-doped silica fiber lasers: versatile sources for the 1-1.2 μm region*, IEEE Journal of Selected Topics in Quantum Electronics **1**(1), 1995, pp. 2–13.

[6] Okhotnikov O.G., Gomes L., Xiang N., Jouhti T., Grudinin A.B., *Mode-locked ytterbium fiber laser tunable in the 980–1070-nm spectral range*, Optics Letters **28**(17), 2003, pp. 1522–1524.

[7] Paschotta R., Nilsson J., Tropper A.C., Hanna D.C., *Ytterbium-doped fiber amplifiers*, IEEE Journal of Quantum Electronics **33**(7), 1997, pp. 1049–1056.

[8] Richardson D.J., Nilsson J., Clarkson W.A., *High power fiber lasers: current status and future perspectives [Invited]*, Journal of the Optical Society of America B **27**(11), 2010, pp. B63–B92.

[9] Hekmat M.J., Dashtabi M.M., Manavi S.R., Hassanpour E., Massudi R., *Selection of suitable pump diode laser parameters and their effects on efficiency and optimum length of Yb-doped double clad fiber lasers*, Laser Physics **22**(10), 2012, pp. 1581–1585.

[10] Dae Seung Moon, Bok Hyeon Kim, Aoxiang Lin, Guoyong Sun, Won-Taek Han, Young-Geun Han, Youngjoo Chung, *Tunable multi-wavelength SOA fiber laser based on a Sagnac loop mirror using an elliptical core side-hole fiber*, Optics Express **15**(13), 2007, pp. 8371–8376.

[11] Kelson I., Hardy A.A., *Strongly pumped fiber lasers*, IEEE Journal of Quantum Electronics **34**(9), 1998, pp. 1570–1577.

[12] KELSON I., HARDY A., *Optimization of strongly pumped fiber lasers*, Journal of Lightwave Technology **17**(5), 1999, pp. 891–897.

[13] LEPROUX P., FÉVRIER S., DOYA V., ROY P., PAGNOUX D., *Modeling and optimization of double-clad fiber amplifiers using chaotic propagation of the pump*, Optical Fiber Technology **7**(4), 2001, pp. 324–339.

[14] KONAK A., COIT D.W., SMITH A.E., *Multi-objective optimization using genetic algorithms: a tutorial*, Reliability Engineering and System Safety **91**(9), 2006, pp. 992–1007.

[15] MINGYI GAO, CHUN JIANG, WEISHENG HU, JINGYUAN WANG, *Optimized design of two-pump fiber optical parametric amplifier with two-section nonlinear fibers using genetic algorithm*, Optics Express **12**(23), 2004, pp. 5603–5613.

[16] SHIJIE ZHENG, NAN ZHANG, YANJUN XIA, HONGTAO WANG, *Research on non-uniform strain profile reconstruction along fiber Bragg grating via genetic programming algorithm and interrelated experimental verification*, Optics Communications **315**, 2014, pp. 338–346.

[17] YULIN LIU, ZEYONG WANG, HONGNA ZHU, XIAORONG GAO, *Gain optimization of fiber optical parametric amplifier based on genetic algorithm with pump depletion*, Applied Optics **52**(31), 2013, pp. 7445–7448.

[18] TAMAKI H., KITA H., KOBAYASHI S., *Multi-objective optimization by genetic algorithms: a review*, Proceedings of IEEE International Conference on Evolutionary Computation, 1996, pp. 517–522.

[19] NILSSON J., JASKORZYNSKA B., *Modeling and optimization of low-repetition-rate high-energy pulse amplification in cw-pumped erbium-doped fiber amplifiers*, Optics Letters **18**(24), 1993, pp. 2099–2101.

[20] ZENTENO L., *High-power double-clad fiber lasers*, Journal of Lightwave Technology **11**(9), 1993, pp. 1435–1446.